OXFORD

SOT | Society of Toxicology
www.toxsci.oxfordjournals.org

TOXICOLOGICAL SCIENCES, 155(1), 2017, 213–223

doi: 10.1093/toxsci/kfw196
Advance Access Publication Date: October 4, 2016
Research article

Manganese Stimulates Mitochondrial H_2O_2 Production in SH-SY5Y Human Neuroblastoma Cells Over Physiologic as well as Toxicologic Range

Jolyn Fernandes, Li Hao, Kaiser M. Bijli, Joshua D. Chandler, Michael Orr, Xin Hu, Dean P. Jones, and Young-Mi Go[1]

Division of Pulmonary, Allergy and Critical Care Medicine, Department of Medicine, Emory University, Atlanta, Georgia 30322

[1]To whom correspondence should be addressed at 205 Whitehead Research Center, Atlanta, GA 30322. Fax: 404-712-2974. E-mail: ygo@emory.edu.

ABSTRACT

Manganese (Mn) is an abundant redox-active metal with well-characterized mitochondrial accumulation and neurotoxicity due to excessive exposures. Mn is also an essential co-factor for the mitochondrial antioxidant protein, superoxide dismutase-2 (SOD2), and the range for adequate intake established by the Institute of Medicine Food and Nutrition Board is 20% of the interim guidance value for toxicity by the Agency for Toxic Substances and Disease Registry, leaving little margin for safety. To study toxic mechanisms over this critical dose range, we treated human neuroblastoma SH-SY5Y cells with a series of $MnCl_2$ concentrations (from 0 to 100 μM) and measured cellular content to compare to human brain Mn content. Concentrations ≤10 μM gave cellular concentrations comparable to literature values for normal human brain, whereas concentrations ≥50 μM resulted in values comparable to brains from individuals with toxic Mn exposures. Cellular oxygen consumption rate increased as a function of Mn up to 10 μM and decreased with Mn dose ≥50 μM. Over this range, Mn had no effect on superoxide production as measured by aconitase activity or MitoSOX but increased H_2O_2 production as measured by MitoPY1. Consistent with increased production of H_2O_2, SOD2 activity, and steady-state oxidation of total thiol increased with increasing Mn. These findings have important implications for Mn toxicity by re-directing attention from superoxide anion radical to H_2O_2-dependent mechanisms and to investigation over the entire physiologic range to toxicologic range. Additionally, the results show that controlled Mn exposure provides a useful cell manipulation for toxicological studies of mitochondrial H_2O_2 signaling.

Key words: cellular redox state; mitochondrial oxidant; MnSOD; neurotoxicity.

Mn is the 12th most abundant mineral element on the earth and is both nutritionally essential and toxic in excess. Mn is required for a number of biological processes including biosynthesis and metabolism of lipids, carbohydrates, and amino acids, and is a cofactor for a diverse set of enzymes (Burton and Guilarte, 2009; Takeda, 2003). Mn concentrations in human brain spans from a normal range at 20.0–52.8 μM Mn (5.3–14.0 ng/mg protein) to toxic range at 60.1–158.4 μM Mn (16–42.1 ng/mg protein) based on extrapolation of studies done in astrocytes and human brain samples (Bowman and Aschner, 2014). Exposure to elevated Mn levels induces cognitive and behavioral deficits resulting in a neurological syndrome similar to Parkinson's disease (Aboud *et al.*, 2012; Bouchard *et al.*, 2011; Kwakye *et al.*, 2015; Menezes-Filho *et al.*, 2011; Myers *et al.*, 2009).

Mn toxicity from occupational exposures is well documented and appropriate hygiene policies are established to avoid health risks (ATSDR, 2012). Emerging evidence suggests, however, that environmental exposures could also pose a threat. Mn exposure can occur through recycling waste, agricultural agents, fuel combustion, natural or anthropogenic contaminations of soil, and water, as well as contaminated foods, infant formulas, food, and nutritional products (ATSDR, 2012;

Golub *et al.*, 2005; Loranger *et al.*, 1994; O'Neal and Zheng, 2015; Roede *et al.*, 2011). Multiple epidemiological studies show neurological effects of exposure to Mn in the workplace using multiple neurobehavioral tests of cognition, mood and neuro-motor activities (Beuter *et al.*, 1999; Bouchard *et al.*, 2005; Lucchini *et al.*, 1995; Standridge *et al.*, 2008; Wasserman *et al.*, 2006). The effects of Mn can be biphasic as seen in a longitudinal study of early life Mn exposure that examined neurodevelopment endpoints at 12 and 36 months of age. The study observed an inverted U-shaped dose-response curve for the effects of Mn exposure on neurodevelopment score suggesting that both high and low Mn exposure can negatively influence child neurodevelopment (Claus Henn *et al.*, 2010).

The nutritional requirement for Mn has been examined in detail by the Food and Nutrition Board (FNB) of the Institute of Medicine (National Academy of Sciences, 2001). Adequate intake (AI) levels were established as 2.3 and 1.8 mg Mn/day, respectively, for men and women. Literature for toxic levels of Mn was examined in detail by the Agency for Toxic Substances and Disease Registry (ATSDR) and no Minimal Risk Levels were established for acute, intermediate or chronic oral exposure to inorganic Mn (ATSDR, 2012). Commonly used methods for extrapolation from animal studies were inconsistent with the FNB values and the ATSDR recommended an interim guidance value for Mn of 0.16 mg/kg/day (ATSDR, 2012). For a 70 kg individual, the resulting interim guidance intake of 11.2 mg/day is less than 5-fold the adequate intake level for men. This narrow range between adequate intake and possible toxic levels emphasizes a critical need to improve understanding of the modes of action and metabolic consequences of Mn over this relevant exposure range.

Whereas the exact mechanism of Mn toxicity is still not known, one proposed mechanism for high dose Mn induced neurotoxicity is oxidative damage, mitochondrial dysfunction, and the resultant apoptotic cell death (Anantharam *et al.*, 2002; Galvani *et al.*, 1995; Gavin *et al.*, 1992; Maddirala *et al.*, 2015; Milatovic *et al.*, 2009; Oubrahim *et al.*, 2001; Yoon *et al.*, 2011; Zhang *et al.*, 2004). Among the Mn induced redox regulated mitochondrial dysfunction, a majority of the studies have been performed in isolated mitochondria from cells treated with Mn or isolated mitochondria stimulated directly by exogenously added Mn to determine the effect of Mn on mitochondrial respiration (Galvani et al., 1992, 1995; Liu *et al.*, 2013). As such, subtle changes in mitochondrial redox may be lost with low physiological Mn dose, because extracellular changes influence mitochondrial redox state.

A study in HeLa cells demonstrated production of cellular reactive oxygen species and apoptosis after treatment with 0.5–2 mM $MnCl_2$ for 24 h (Oubrahim *et al.*, 2001). Another study reported increased cellular oxidant production and decreased ATP production on treatment with 0.8 mM $MnCl_2$ for 24 h in SH-SY5Y cells (Maddirala *et al.*, 2015). Other studies showed Mn-dependent inhibition of mitochondrial Complex I in PC12 cell cultures (Galvani *et al.*, 1995) and inhibition of ATP synthesis in isolated mitochondria *in vitro* (Gavin *et al.*, 1992). Most of these studies have determined outcomes following relatively high level acute or chronic exposure to Mn (Aschner *et al.*, 2005), and less is known about the effects or thresholds of Mn at levels activating cellular and mitochondrial redox signaling. Moreover, what aspect of mitochondrial redox signaling and generation of which oxidant species is altered under physiological and toxicological concentration of Mn still remains unclear. An understanding of redox responses to Mn doses approximating real-life exposures and defining oxidant species and source could help recognize possible risks due to interactions with other toxicological stressors and in physiologic adaptation.

Briefly our study showed lower concentrations of Mn in the culture medium resulted in low cellular Mn (physiological; $\leq 15.7 \pm 1.1$ ng/mg protein) and stimulated mitochondrial respiration whereas higher cellular Mn (toxicological; $>36.77 \pm 1.83$ ng/mg protein) inhibited mitochondrial respiration and caused cellular thiol oxidation. Results showed that superoxide dismutase 2 (SOD2) activity, was increased by Mn, that no increase in superoxide anion production was detected and that increased H_2O_2 production occurred as a function of Mn over the entire physiologic and toxicological range.

MATERIALS AND METHODS

Cell culture and Mn treatment. The human neuroblastoma cell line SH-SY5Y was obtained from the American Type Culture Collection (ATCC-Manassas, Virginia), and maintained in medium consisting of Dulbecco's Modified Eagle Medium/Ham's F12 medium (1:1 mixture), 10% FBS, and 1% penicillin, and streptomycin. This cell line was selected as an experimental model that exhibits characteristics similar to neuronal cells and possesses dopaminergic neuronal markers (Gordon *et al.*, 2013; Kovalevich and Langford, 2013; Xie *et al.*, 2010). SH-SY5Y cells have been extensively characterized as an *in vitro* human cell model for neurodegenerative diseases including Parkinson's Disease and Alzheimer's Disease, and for mitochondrial dysfunction and neuronal cell death induced by oxidative stress (Gao *et al.*, 2001; Wu *et al.*, 2014; Zhu *et al.*, 2007). All assays were conducted within 10 cell passages. The cells were treated with $MnCl_2$ (Sigma, indicated as Mn in following sections) at varying concentrations (0, 1, 5, 10, 50, and 100 μM) for 5 h. For all experimental conditions, serum was reduced to 0.5% FBS. These conditions were selected because there was no cell death at 5 h but after return of cells to culture medium for 24 or 48 h, cells exposed to ≤ 10 μM Mn for 5 h survived whereas cells exposed to ≥ 50 μM had substantial cell death.

Cellular Mn concentration measurement. Intracellular Mn^{2+} concentrations were measured by graphite furnace atomic absorption spectroscopy (GFAA) (Thermo Scientific iCE3000 Series). Briefly, following treatment with Mn, SH-SY5Y cells were washed 3 times with phosphate buffered saline (PBS) and resuspended in ultrapure cell culture grade water. The cells were then lysed by repeated freeze thawing cycles followed by sonication and frozen at −80°C for further analysis.

Total cellular thiol. Following Mn treatment, cells were washed 3 times with PBS, harvested with ice cold PBS with 0.5% Triton X-100 and centrifuged at 10 000 × *g* for 10 min. Ellman's reagent (5,5′-dithio-bis-[2-nitrobenzoic acid]) (1 mM) in 100 mM potassium phosphate buffer with 1 mM EDTA at pH 7.5 was added to the cell lysates and incubated for 5 min in the dark (Chandler *et al.*, 2013). Total thiol content was measured at an absorbance of 412 nm and lysate-free buffer as a blank. Final values were expressed relative to the protein content measured for each sample.

GSH and GSSG. At the end of the treatment period, the cells were washed 3 times with PBS. Five hundred microliters of ice cold 5% perchloric acid, 0.2 M boric acid, and 10 μM γ-glutamylglutamate was added to each plate, and the cells were scraped and collected

in tubes placed on ice. Samples were then derivatized with iodoacetic acid followed by derivatization with dansyl chloride, and analyzed by high performance liquid chromatography (HPLC) with fluorescence detection to determine the GSH and GSSG concentrations (Jones, 2002; Jones *et al.*, 1998).

Mitochondrial function analysis. Following 5 h treatment, the media was replaced with fresh media containing the WST-1 reagent (Roche) to determine mitochondrial function. The assay is based on the cleavage of the tetrazolium salt WST-1 to formazan by cellular mitochondrial dehydrogenases. The plate was then incubated for 1 h at 37 °C and absorbance was read at 450 nm on a microplate reader (Spectramax M2).

Intracellular mitochondrial oxidant level analysis. To evaluate mitochondrial oxidant generation, multiple assays were employed. For detection of global mitochondrial oxidation, Mn treated cells were incubated with Mitotracker Red CM-H2XRos, and mitotracker fluorescence as a measure of mitochondrial oxidant generation was visualized by fluorescence microscopy as previously described (Go *et al.*, 2010). For a more specific mitochondrial oxidant marker, superoxide anion measurement was performed using MitoSOX (5 μM, Invitrogen) as described previously (Go *et al.*, 2009). For mitochondrial H_2O_2 measurement, live cell imaging was performed using Mitochondrial peroxy yellow 1 (MitoPY1) (10 μM, Tocris Biosciences) based on the protocol previously described (Lippert *et al.*, 2015).

Cellular respiration. Oxygen consumption rate (OCR) and extracellular acidification rate (ECAR) were measured using a Seahorse Bioscience XF96 extracellular flux analyzer (North Billerica, Massachusetts). Plates were seeded at 40 000 cells/well. After 24 h, cells were treated with graded concentrations of Mn (0, 1, 5, 10, 50, and 100 μM) in DMEM medium containing 0.5% fetal bovine serum for 5 h. Cells were then washed 3 times with prewarmed serum-free DMEM media. Cells were incubated with XF assay media (pH 7.4, Seahorse Biosciences) supplemented with 10 mM glucose, 1 mM sodium pyruvate, and 2 mM L-glutamine using the XF Prep Station (Seahorse Bioscience). Cells were incubated for 1 h at 37 °C without CO_2. The inhibitors of mitochondrial respiration, including oligomycin at 1 μM, rotenone at 1 μM, and FCCP at 1 μM were auto-injected into the experimental wells (based on optimization experiments). Each experimental point is an average of a minimum of 10 replicate wells and each experiment was performed 3 times with different plates. Data were reported as OCR or ECAR values normalized to initial number of plated cells or as percentage of the time point for no manganese treated control group.

SOD activity. Cells were washed 3 times with PBS and total SOD activity measurements were performed spectrophotometrically with a xanthine oxidase-based assay according to the manufacturer's instructions (Cayman Chemical). Rates were calibrated relative to the SOD standard provided with the kit. Measurements of SOD2 activity were obtained with an in-gel nitroblue tetrazolium assay using native gels as described previously (Van Remmen *et al.*, 1999). Results are expressed relative to control cells.

Statistical analysis. Statistics were performed using the software package GraphPad Prism version 6 (GraphPad Software, LaJolla, California). Data were analyzed using 1-way analysis of variance (ANOVA). Data in graphs were represented as the mean ± SE. Statistically significant differences are defined as P values $<.05$ between control and each treatment and denoted with an asterisk (*) throughout.

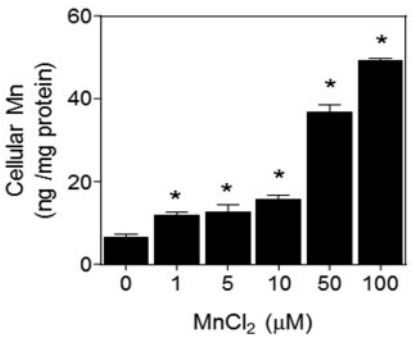

FIG. 1. Dose-dependent increase in cellular Mn in human neuroblastoma cells. SH-SY5Y cells treated with varying concentrations of $MnCl_2$ (0, 1, 5, 10, 50, and 100 μM) for 5 h were measured for their cellular Mn content using Graphite Furnace Atomic Adsorption Spectrometer (GFAA). Results are shown as mean ± SE ($n = 3$). *$P < .05$ compared with control (No Mn treatment).

RESULTS

Mn Accumulates in Human SH-SY5Y Cells in a Dose-Dependent Manner and Represents Physiological to Pathological Ranges Found in Human Brain Tissue

To establish a cellular model that represents Mn concentrations over a physiological to a minimally toxicological range, SH-SY5Y cells treated with different Mn doses for 5 h were examined for Mn content and compared with the previously reported Mn levels in human brain tissues (Figure 1). Results showed that cellular Mn increased in a dose-dependent manner [0 μM, 6.4 ± 1.0 ng Mn/mg protein; 1 μM, 12.0 ± 0.7 ng Mn/mg protein; 5 μM, 12.7 ± 1.8 ng Mn/mg protein; 10 μM, 15.7 ± 1.1 ng Mn/mg protein; 50 μM, 36.8 ± 1.8 ng Mn/mg protein; 100 μM, 49.2 ± 0.5 ng Mn/mg protein]. The data show that cellular Mn in response to ≤10 μM Mn treatment was within the range found in human brain tissues at physiological conditions (Bowman and Aschner, 2014; Csaszma *et al.*, 2003), whereas cellular Mn in response to ≥50 μM Mn treatment were comparable to Mn tissue concentrations found in pathophysiological conditions (Bowman and Aschner, 2014; Erikson *et al.*, 2007; Molina *et al.*, 2011). The intracellular content of Mn in control SH-SY5Y cells (No Mn treatment group) was less than 8% of the lowest exogenously added Mn treatment group (1 μM $MnCl_2$) and likely was derived from FBS in growth media and treatment media (Cho *et al.*, 2007).

Mn-Stimulated Oxidation of Cellular Redox State Occurs without Triggering Cytotoxic Signaling

To examine cellular responses to Mn concentrations, from nontoxic to toxic range, we examined the cellular redox state and mitochondrial function of SH-SY5Y cells. The effect of Mn on total thiol, glutathione and glutathione disulfide levels were quantified after 5 h treatment with Mn, using Ellman's reagent and HPLC analyses, respectively. The results showed that Mn treatment significantly decreased total cellular thiol in a dose dependent manner, thereby presenting evidence for oxidative stress [1 μM, 91.9 ± 4.4%; 5 μM, 88.7 ± 3.0%; 10 μM, 86.8 ± 3.4%; 50 μM, 83.1 ± 5.6%; 100 μM, 81.4 ± 0.8% compared with control at 100%] (Figure 2A). In addition, the analysis of the major cellular thiol/disulfide redox couple (GSH and GSSG) demonstrated a significant increase in glutathione disulfide (GSSG) with 100 μM $MnCl_2$ treatment [0 μM, 0.12 ± 0.02 mM; 1 μM, 0.14 ± 0.00 mM;

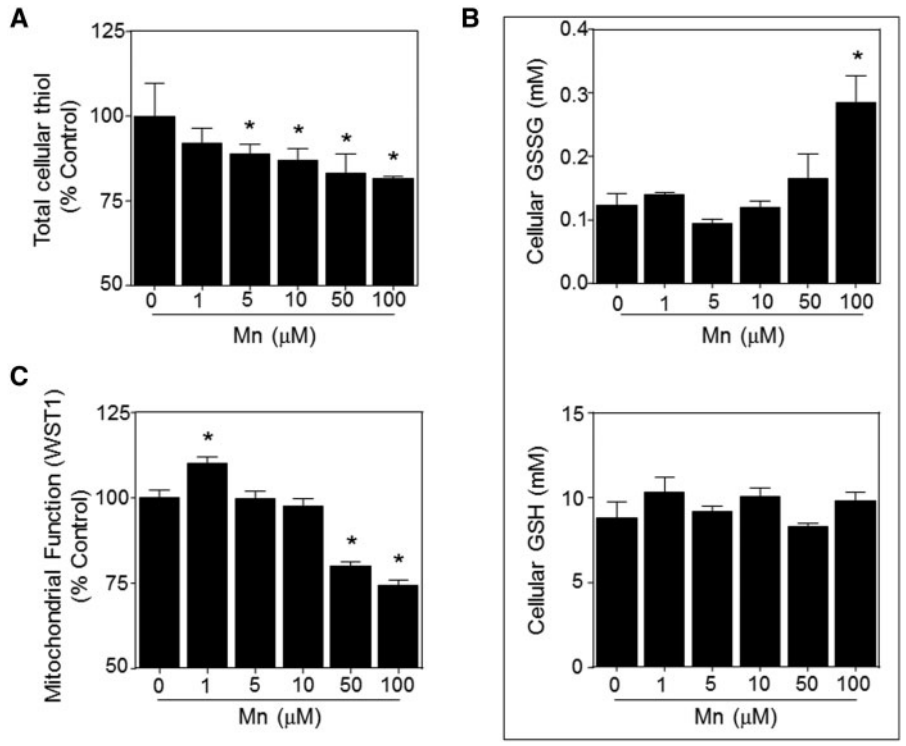

FIG. 2. Effect of Mn on the cellular redox status and mitochondrial function of SH-SY5Y cells. (A) Cells were treated for 5 h with $MnCl_2$ concentrations as indicated, and total cellular thiol content was quantified spectrophotometrically with Ellman's reagent. (B) Cellular glutathione disulfide (GSSG) and glutathione (GSH) were determined by fluorescence following derivatization with dansyl chloride and HPLC separation. Corresponding redox potential values are provided in Supplementary Figure 1. (C) Mitochondrial dehydrogenase activity was measured using WST-1 dependent colorimetric assay. Under these conditions, there was no loss in cell viability as measured by Trypan Blue staining, shown in Supplementary Figure 2, or increase in apoptosis signaling, shown in Supplementary Figure 3. Results are shown as mean ± SE ($n \geq 3$). *$P < .05$ compared with control (No Mn treatment).

5 μM, 0.09 ± 0.01 mM; 10 μM, 0.12 ± 0.01 mM; 50 μM, 0.16 ± 0.04 mM; 100 μM, 0.28 ± 0.04 mM GSSG] (Figure 2B, top), whereas no detectable effect on glutathione (GSH) was observed (Figure 2B, bottom). Consistent with evidence for oxidative stress, the calculated redox potential was more oxidized at ≥ 50 μM Mn treatment (Supplementary Figure 1). Subsets of cells treated with Mn were analyzed for cytotoxicity and the results of trypan blue and cytochrome c release showed that even the highest dosage of Mn (100 μM Mn treatment for 5 h) had no effect on cell viability or apoptotic events at this time point (Supplementary Figs. 2 and 3), suggesting that oxidative cellular signaling responses occur prior to any observable cytotoxic events by Mn exposure.

Mitochondria are an important source of oxidants (Apostolova and Victor, 2015; Lin and Beal, 2006; Nemoto *et al.*, 2000), and prior research shows that Mn mainly accumulates in the mitochondria (Gavin *et al.*, 1999; Maynard and Cotzias, 1955). To determine effects of Mn dose on viable cell activity, we used WST-1 a tetrazolium dye that is reduced by NAD(P)H-linked dehydrogenases in living cells. Results showed an increased activity at 1 μM (110.0 ± 1.9% of control) and significantly decreased values at 50 and 100 μM [50 μM, 79.9 ± 1.4%; 100 μM, 74.2 ± 1.7% compared with control] (Figure 2C).

Dose-Dependent Biphasic Effects of Mn on Mitochondrial Respiration

To determine the effect of Mn concentrations on mitochondrial respiratory function, we measured oxygen consumption rate (OCR) in SH-SY5Y cells following 5 h Mn treatment using Seahorse XF96 Extracellular Flux Analyzer. Results showed that ≤50 μM Mn increased OCR relative to control (1 μM, 121 ± 7%; 5 μM, 124 ± 6%; 10 μM, 126 ± 9%; 50 μM, 129 ± 9%; Figure 3A) whereas 100 μM Mn was not different from control (96 ± 6% OCR compared with control; Figure 3A). Mitochondrial OCR declined further (50–70% of control values) with concentrations above 100 μM Mn (data not shown).

In the Seahorse analyses, Mn treated cells were treated sequentially with oligomycin to determine ATP-linked OCR and rotenone to determine proton-leak dependent OCR. ATP-linked oxygen consumption did not change with increasing Mn concentration up to 100 μM Mn treatment (Figure 3B). Proton-leak dependent OCR was increased relative to basal OCR at Mn concentrations up to 50 μM (1 μM, 140 ± 14%; 5 μM, 149 ± 11%; 10 μM, 169 ± 20%; 50 μM, 149 ± 14%) but was not different from control at 100 μM (105 ± 10%) (Figure 3C). A 4 quadrant metabolic profile graph of the relative mitochondrial (OCR) and glycolytic metabolism (ECAR) at the different Mn treatment dosage (Figure 3D) shows that the lower concentrations of Mn stimulate both glycolysis and mitochondrial respiration: mitochondrial respiration (OCR) declines at Mn concentrations above 10 μM Mn treatment whereas glycolysis (ECAR) does not decline except at 100 μM Mn.

Mn Treatment Increases H_2O_2 Production in the Mitochondria

Whereas alterations in the mitochondrial respiration are a major source of oxidant production, generation of mitochondrial oxidants also disrupts mitochondrial and cellular function (Adam-Vizi, 2005; Bao *et al.*, 2009; Kowaltowski *et al.*, 2009). To determine mitochondrial oxidant production in Mn-treated cells, we used multiple mitochondria-specific fluorescent probes. MitoTracker red CM-H_2XRos (MitoTracker) is a commonly used probe that provides information on oxidant production and

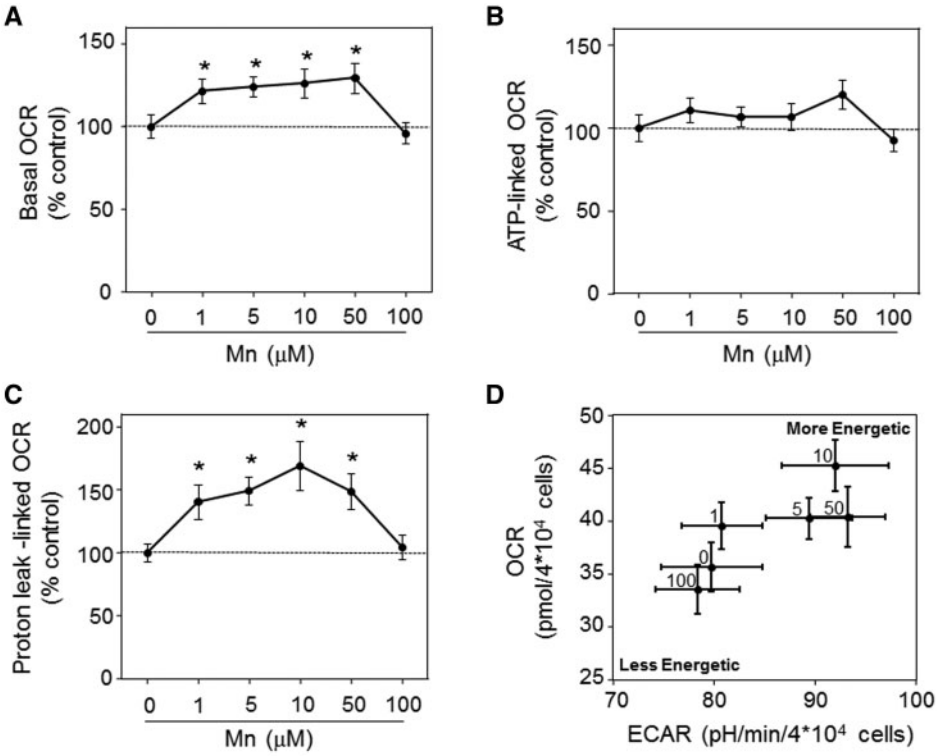

FIG. 3. Low dose Mn effects on mitochondrial and glycolytic activities of SH-SY5Y cells using Seahorse XF96 extracellular flux analyzer. Cells were treated for 5 h with Mn at concentrations indicated. (A) Basal mitochondrial oxygen consumption rate (OCR) as a percentage of control without added Mn. (B) OCR related to ATP-synthesis measured after addition of oligomycin. (C) OCR linked to proton leak measured after the addition of FCCP. (D) Relative effects of different concentrations of Mn on mitochondrial and glycolytic activities were visualized by plotting OCR as a function of ECAR, where each is expressed as a function of OCR without inhibitor. Labels for Mn concentrations are given adjacent to each data point. Data are presented as mean ± SE for 3 separate experiments, where each experiment had ≥10 replicate wells per treatment. *$P < .05$ versus control group.

redox status but is relatively nonspecific (Dikalov and Harrison, 2014; Karlsson *et al.*, 2010; Winterbourn, 2014). In contrast, MitoSOX is relatively specific for superoxide anion radical and MitoPY1 is a boronate-based probe (Kaludercic *et al.*, 2014) that is relatively specific for H_2O_2. MitoTracker florescence increased with Mn dose (Figure 4A), with statistically significant increases observed at 10 μM and higher (1 μM, 113 ± 6%; 5 μM, 127 ± 7%; 10 μM, 134 ± 6%; 50 μM, 147 ± 7%; 100 μM, 154 ± 7% compared with control at 100%; Figure 4B). MitoSOX did not show any observable oxidation, even though positive controls with antimycin A showed increase; thus, the results show no observable effects on mitochondrial superoxide production at all the concentrations tested (data not shown). In contrast, MitoPY1 fluorescence increased as a function of Mn (Figure 5A), with significant increase at 10 μM and higher (1 μM, 133 ± 20%; 5 μM, 140 ± 32%; 10 μM, 157 ± 18%; 50 μM, 196 ± 33%; 100 μM, 197 ± 17% compared with control at 100%; Figure 5B). This increase in mitochondrial H_2O_2 measured by MitoPY1 is consistent with the results obtained from Mitotracker. Thus, the results show that mitochondrial H_2O_2 production in SH-SY5Y is increased by Mn over the entire physiologic to toxicologic range studied.

Mn Increases Mitochondrial Superoxide Dismutase Activity

Superoxide dismutase (SOD2), found in the mitochondrial matrix, converts superoxide to oxygen and hydrogen peroxide. Mn is a cofactor for SOD2 and is critical for SOD2 activity. Total SOD activity was elevated approximately 25% compared with the controls at all Mn concentrations (0 μM, 4.4 ± 0.2; 1 μM, 5.5 ± 0.7; 5 μM, 5.7 ± 0.5; 10 μM, 5.3 ± 0.3; 50 μM, 6.4 ± 0.9; 100 μM, 6.2 ± 0.7 U/mg protein; Figure 6A). Consistent with the data for total SOD, Mn dose-dependent increase in SOD2 activity was also observed [1 μM, 111 ± 1; 5 μM, 118 ± 15%; 10 μM, 124 ± 9%; 50 μM, 133 ± 17%; 100 μM, 147 ± 13% compared with control at 100%; Figure 6B).

DISCUSSION

Aberrant brain Mn levels have been associated with Manganism, Parkinsonism and other neurological problems (Kwakye et al., 2015; Menezes-Filho et al., 2011; O'Neal and Zheng, 2015). However, in most studies, the lack of measure of the intracellular Mn levels that lead to molecular derangements have hindered our understanding of the effects of Mn within a physiological and pathological setting. Mn is a redox active metal, and little is known about the mitochondrial-cellular redox signaling resulting in differential cellular response to low dose acute Mn exposure. Multiple studies determining subcellular Mn distribution in organs and intracellular organelles *in vivo* have demonstrated dosage dependent increases in intramitochondrial Mn (Ayotte and Plaa, 1985; Lai *et al.*, 1999; Liccione and Maines, 1988; Maynard and Cotzias, 1955; Miller *et al.*, 1975), suggesting a direct association of mitochondrial responses with Mn levels. The present study builds upon this earlier research by measuring cellular Mn concentrations and associated effects on cellular redox states and mitochondrial oxidant production and respiration, specifically under conditions that differ in effects on cell survival. Important differences

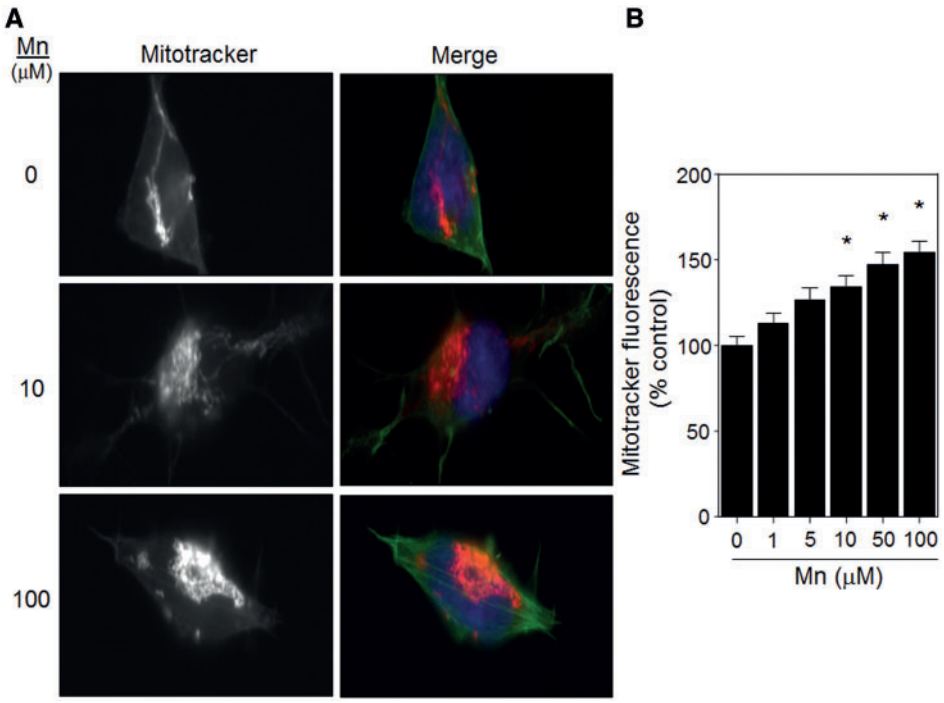

FIG. 4. Mn-dependent increase in mitochondrial oxidant levels measured by Mitotracker Red CM-H_2XRos. (A) Right panels show mitochondrial oxidant (red) levels visualized by fluorescence microscopy using mitotracker red CM-H_2XRos, with Hoechst (blue) staining for nuclei and Phallacidin (green) staining for F-actin. The left panels show the relative intensities for the mitotracker fluorescence alone. (B) Mean fluorescence intensity of each group was determined and plotted as relative % increase compared with control group (0 μM Mn treatment). The data are shown as mean ± SE ($n \geq 5$). *$P < .05$ versus control group.

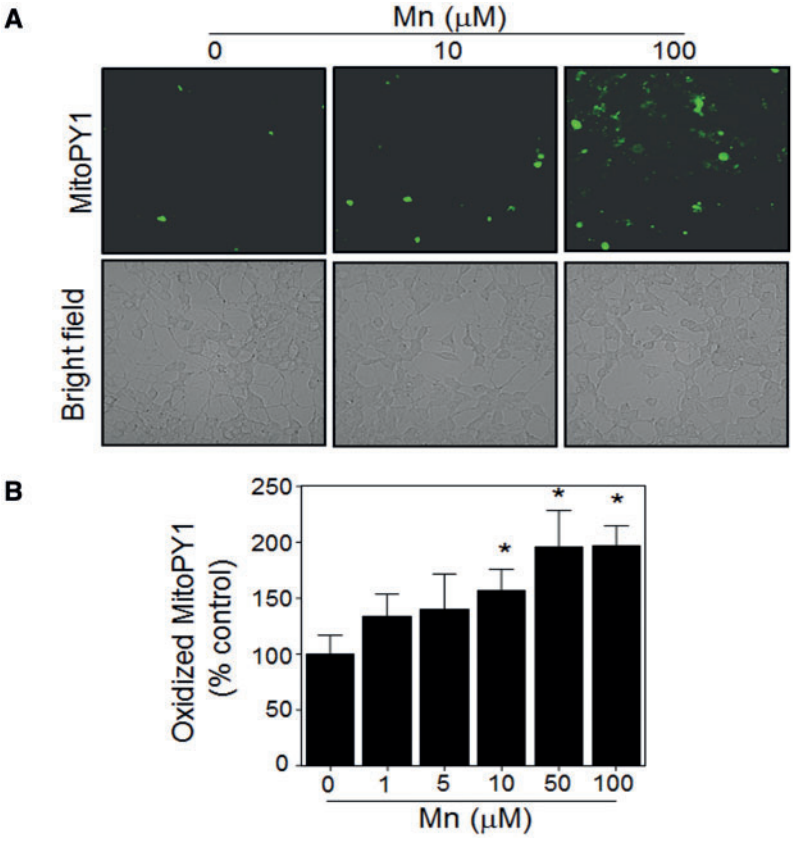

FIG. 5. Mn-dependent increase in mitochondrial H_2O_2 production measured by MitoPY1. (A) Live cell mitochondrial H_2O_2 production was visualized by fluorescence microscopy using MitoPY1 (green) and bright field. (B) Mean fluorescence intensity for each group was determined and plotted as relative % increase compared with control group (0 μM Mn treatment). The data are shown as mean ± SE ($n \geq 5$). *$P < .05$ versus control group.

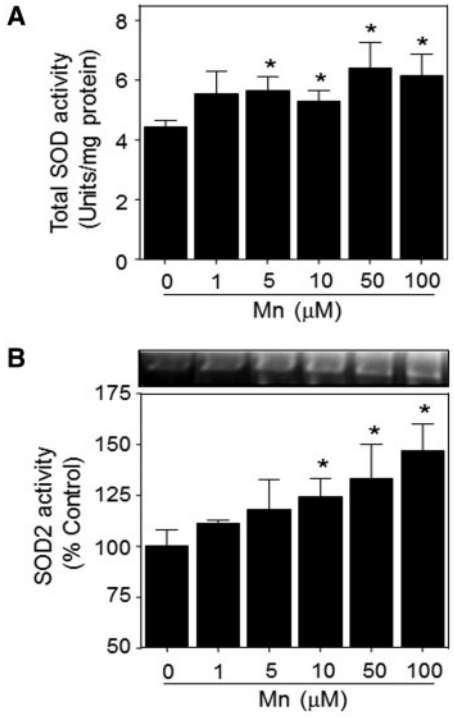

FIG. 6. Superoxide dismutase enzyme activity following Mn treatment. (A) SOD activity in SH-SY5Y cells was measured by a colorimetric assay in whole cell lysate following treatment with respective $MnCl_2$ concentration for 5 h. (B) SOD2 enzyme activity in native gels was analyzed by nitroblue tetrazolium-based assay (top panel) and relative intensities of bands were obtained by densitometry analysis and plotted as a function of the control group. The entire gel is shown in Supplementary Figure 4. The data are shown as mean ± SE ($n \geq 3$). *$P < .05$ versus control group (0 μM Mn treatment).

were detected for H_2O_2 production, mitochondrial respiration and thiol oxidation.

The inability to detect an increase in superoxide anion radical production in response to Mn may be particularly important in understanding Mn-dependent toxicity. Prior discussions have addressed differences between radical and nonradical mechanisms of oxidative stress (Jones, 2008), but considerable evidence supports a role for superoxide anion radical in mitochondrial oxidative toxicity. Importantly, Mn is a required component of SOD2, which functions to convert superoxide anion radical, a product of the mitochondrial respiratory chain, to H_2O_2 and O_2. The results with increasing Mn showed no detectable increase in superoxide anion radical as measured by inactivation of aconitase (data not shown) or oxidation of MitoSox. At the same time, increased activity of SOD2 and increased H_2O_2 were observed. Mn commonly occurs in +2 and +4 oxidation states, but +3, +5, and +7 also occur, so one cannot infer predominant electron transfer reactions from the data, ie, superoxide anion radical could be formed and dismutated without a detectable increase, or reactions could occur with 2-e^- transfer to produce H_2O_2 without detectable superoxide anion radical. In either case, an important conclusion is that Mn results in a dose-dependent increase in mitochondrial H_2O_2 production over the entire dose range. These results suggest that variation in Mn in culture media may be an unanticipated variable in cell culture studies. Additionally, the results suggest that controlled variation in Mn could be used to test the involvement of mitochondrial H_2O_2 in toxicity of other agents.

Whereas H_2O_2 is known to cause oxidative stress and toxicity, in the recent years H_2O_2 has also gained interest as a signaling molecule and as a part of normal aerobic metabolism (Bao *et al.*, 2009; Sies, 2014). Whereas determining the H_2O_2 threshold from signaling to excessive toxic levels has been challenging

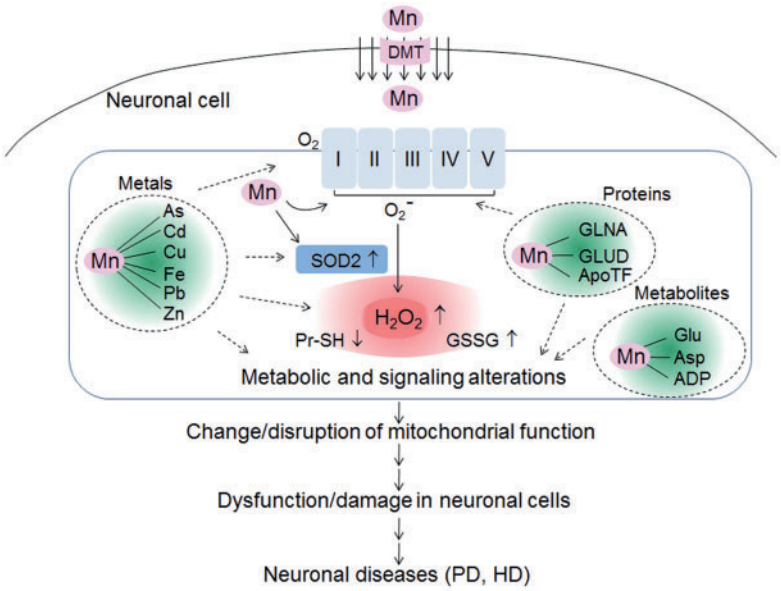

FIG. 7. Central role of mitochondrial H_2O_2 in Mn physiology and toxicity. The present results show that Mn dose-response involves a low-dose activation of respiration and SOD2 activity without associated toxicity whereas further increase in Mn inhibits respiration, oxidizes cell GSH and protein thiols, and causes cell death. Over this entire range, H_2O_2 increases as a function of Mn, suggesting that H_2O_2 has a signaling role at lower Mn concentrations and a toxic role at higher Mn concentration. Elucidation of the interactions of Mn-containing complexes (Mn-metal, Mn-protein, Mn-metabolite, dotted circles) with these central Mn-dependent mitochondrial reactions could considerably enhance understanding of related neuronal disease mechanisms. Abbreviations: Pr-SH, protein thiol; GSSG, glutathione disulfide; DMT, divalent metal transporter; GLNA, glutamine synthetase; GLUD, glutamiate dehydrogenase; ApoTF, apotransferrin; PD, Parkinson's Disease; HD, Huntington's Disease.

(Sies, 2014), evaluation of a system using redox-active chemicals that are endogenously present at sub-toxic concentrations within a cell, such as Mn, sheds light on this threshold concept. Our study shows that Mn increases mitochondrial H_2O_2 over the entire physiological to pathological range studied (Figure 5) whereas GSH oxidation, protein oxidation, WST1 reduction, and mitochondrial respiration were only significantly affected at the higher concentrations. This indicates that the transition from normal to toxic conditions may be better described in terms of the concept of redox optimization (Cortassa *et al.*, 2014) where oxidant generation and elimination are maintained within appropriate ranges.

Our results are consistent with the recommended dosage of treatment and accumulation of Mn within the cells based on relevant *in vivo* levels from human brain studies (Bowman and Aschner, 2014; Csaszma et al., 2003). Total cellular Mn concentration was similar to the physiological and pathophysiological levels of Mn in the human brain. Mn homeostasis in the brain is largely dependent on the circulating pool of Mn wherein the levels in the blood influence the accumulation of Mn in the brain (Bornhorst *et al.*, 2012; Burton and Guilarte, 2009). With the assumption that protein content per cellular volume of neuroblastoma cells is 0.2 mg/μl (Bowman and Aschner, 2014; Matthews, 1974), our data show that 1 μM Mn in the culture medium was associated with cellular value of 12 ± 1 ng/mg protein, which represents the physiological level, whereas 50 μM Mn was associated with 37 ± 2 ng/mg protein, a toxic range 3 times higher than physiological level (Figure 1).

Neurotoxic effects of Mn have been proposed through mitochondrial dysfunction and oxidative stress induced apoptotic cell death (Kitazawa *et al.*, 2002; Milatovic, et al., 2009). Based on our study we determined that cellular Mn 13 ± 2 ng/mg protein (5 μM Mn treatment in Figure 1) causes a 40% increase in mitochondrial H_2O_2 production with no detectable cytotoxicity (5 μM Mn treatment in Supplementary Figure S2). However, higher Mn in cells (37 ± 2 ng/mg protein; 50, 100 μM Mn treatment in Figure 1) led to a 96% increase in oxidant production (Figure 4B) a 20% decline in mitochondrial function (Figure 2C) and subsequent cell death (data not shown). These changes could associate with cytotoxic mechanisms such as cytochrome c release from mitochondria and activation of apoptosis (Yang *et al.*, 1997).

Finally, the relationship of the oxidative mechanisms of inorganic Mn to toxicities of Mn complexes, as summarized in Figure 7, will require further investigation. Previous studies show interaction of Mn with other molecules in toxicological mechanisms (Cui and Okayasu, 2008; Fazakerley and Reid, 1979; Gruden and Munic, 1987; Murthy *et al.*, 1981; Padua *et al.*, 2010; Roney and Colman, 2004). For instance, Mn interactions with toxic heavy metals (As, Cd, Pb), dietary metals (Zn, Mg, Fe, Cu)] (Cui and Okayasu, 2008; Gruden and Munic, 1987; Murthy et al., 1981; Roney and Colman, 2004), proteins (glutamine synthetase, glutamate dehydrogenase, apotransferrin) (Dimovasili *et al.*, 2015; Hunt and Ginsburg, 1981; Yao *et al.*, 2013), and metabolites (glutamate, ADP) (Fazakerley and Reid, 1979; Weiner *et al.*, 1975) have been shown to impact cell physiology. The mechanisms of these effects on neuronal metabolism, signaling and toxicity are largely unknown and may involve interactions of Mn complexes as well as direct Mn effects on respiration and H_2O_2 production (Figure 7). Evidence that Parkinson's disease susceptibility genes are involved in Mn homeostasis further suggests that complex cell-specific mechanisms may be important in Mn toxicity. Parkinson's disease associated genes *ATP13A2*, *parkin*, *DJ-1*, and *α-synuclein* have been shown to be involved in Mn transport and Mn toxicity (Bornhorst *et al.*, 2014; Gitler *et al.*, 2009). Therefore combined studies of gene expression and metabolism associated with Mn effects will be needed to understand complex mitochondria-cellular signaling responses that could protect or exacerbate the Mn-related neurological disorders.

In summary, the present results show that the redox-active essential nutrient, Mn, impacts redox processes in neuroblastoma cell mitochondria over the entire range corresponding to physiological and toxicological concentrations in human brain. Among possible reactive oxygen species, evidence with selective mitochondrial fluorescent probes shows that H_2O_2 is increased in response to increased Mn. This indicates that H_2O_2 may have a signaling role in cellular homeostasis in addition to a role in toxicity at higher Mn concentrations. Finally, the biphasic nature of Mn effects on mitochondrial respiration, when coupled to increased H_2O_2 generation and altered thiol antioxidant systems, may require an integrated systems approach to fulfill dietary requirements whereas avoiding adverse effects from excess Mn exposure.

SUPPLEMENTARY DATA

Supplementary data are available online at http://toxsci.oxfordjournals.org/.

ACKNOWLEDGMENTS

Drs Young-Mi Go and Dean P. Jones share equal senior authorship in this collaborative research. The authors gratefully acknowledge the help of Bonnie Lyon, PhD and Kurt Pennell, PhD, from Tufts University for their technical assistance with Mn measurement on Graphite furnace atomic adsorption spectrometer.

FUNDING

NIEHS Grant R01 ES023485 (to D.P.J. and Y.M.G.) and R21 ES025632 (to D.P.J. and Y.M.G.); NIH S10 OD018006 (to D.P.J.); Cystic Fibrosis Foundation CHANDL16F0 (to J.D.C.).

REFERENCES

Aboud, A. A., Tidball, A. M., Kumar, K. K., Neely, M. D., Ess, K. C., Erikson, K. M., and Bowman, A. B. (2012). Genetic risk for Parkinson's disease correlates with alterations in neuronal manganese sensitivity between two human subjects. *Neurotoxicology* **33**, 1443–1449.

Adam-Vizi, V. (2005). Production of reactive oxygen species in brain mitochondria: Contribution by electron transport chain and non-electron transport chain sources. *Antioxid. Redox Signal.* **7**, 1140–1149.

Anantharam, V., Kitazawa, M., Wagner, J., Kaul, S., and Kanthasamy, A. G. (2002). Caspase-3-dependent proteolytic cleavage of protein kinase Cdelta is essential for oxidative stress-mediated dopaminergic cell death after exposure to methylcyclopentadienyl manganese tricarbonyl. *J. Neurosci.* **22**, 1738–1751.

Apostolova, N., and Victor, V. M. (2015). Molecular strategies for targeting antioxidants to mitochondria: Therapeutic implications. *Antioxid. Redox Signal.* **22**, 686–729.

Aschner, M., Erikson, K. M., and Dorman, D. C. (2005). Manganese dosimetry: Species differences and implications for neurotoxicity. *Crit. Rev. Toxicol.* **35**, 1–32.

ATSDR. (2012). Toxicological Profile for Manganese.United States Department of Health and Human Services, Public Health

Service, Agency for Toxic Substances and Disease Registry, Atlanta, GA.

Ayotte, P., and Plaa, G. L. (1985). Hepatic subcellular distribution of manganese in manganese and manganese-bilirubin induced cholestasis. *Biochem. Pharmacol.* **34**, 3857–3865.

Bao, L., Avshalumov, M. V., Patel, J. C., Lee, C. R., Miller, E. W., Chang, C. J., and Rice, M. E. (2009). Mitochondria are the source of hydrogen peroxide for dynamic brain-cell signaling. *J. Neurosci.* **29**, 9002–9010.

Beuter, A., Edwards, R., deGeoffroy, A., Mergler, D., and Hundnell, K. (1999). Quantification of neuromotor function for detection of the effects of manganese. *Neurotoxicology* **20**, 355–366.

Bornhorst, J., Chakraborty, S., Meyer, S., Lohren, H., Brinkhaus, S. G., Knight, A. L., Caldwell, K. A., Caldwell, G. A., Karst, U., Schwerdtle, T., *et al.* (2014). The effects of pdr1, djr1.1 and pink1 loss in manganese-induced toxicity and the role of alpha-synuclein in *C. elegans*. *Metallomics* **6**, 476–490.

Bornhorst, J., Wehe, C. A., Huwel, S., Karst, U., Galla, H. J., and Schwerdtle, T. (2012). Impact of manganese on and transfer across blood-brain and blood-cerebrospinal fluid barrier in vitro. *J. Biol. Chem.* **287**, 17140–17151.

Bouchard, M., Mergler, D., and Baldwin, M. (2005). Manganese exposure and age: Neurobehavioral performance among alloy production workers. *Environ. Toxicol. Pharmacol.* **19**, 687–694.

Bouchard, M. F., Sauve, S., Barbeau, B., Legrand, M., Brodeur, M. E., Bouffard, T., Limoges, E., Bellinger, D. C., and Mergler, D. (2011). Intellectual impairment in school-age children exposed to manganese from drinking water. *Environ. Health Perspect.* **119**, 138–143.

Bowman, A. B., and Aschner, M. (2014). Considerations on manganese (Mn) treatments for in vitro studies. *Neurotoxicology* **41**, 141–142.

Burton, N. C., and Guilarte, T. R. (2009). Manganese neurotoxicity: Lessons learned from longitudinal studies in nonhuman primates. *Environ. Health Perspect.* **117**, 325–332.

Chandler, J. D., Nichols, D. P., Nick, J. A., Hondal, R. J., and Day, B. J. (2013). Selective metabolism of hypothiocyanous acid by mammalian thioredoxin reductase promotes lung innate immunity and antioxidant defense. *J. Biol. Chem.* **288**, 18421–18428.

Cho, Y. E., Lomeda, R. A., Ryu, S. H., Lee, J. H., Beattie, J. H., and Kwun, I. S. (2007). Cellular Zn depletion by metal ion chelators (TPEN, DTPA and chelex resin) and its application to osteoblastic MC3T3-E1 cells. *Nutr. Res. Pract.* **1**, 29–35.

Claus Henn, B., Ettinger, A. S., Schwartz, J., Tellez-Rojo, M. M., Lamadrid-Figueroa, H., Hernandez-Avila, M., Schnaas, L., Amarasiriwardena, C., Bellinger, D. C., Hu, H., *et al.* (2010). Early postnatal blood manganese levels and children's neurodevelopment. *Epidemiology* **21**, 433–439.

Cortassa, S., O'Rourke, B., and Aon, M. A. (2014). Redox-Optimized ROS Balance and the relationship between mitochondrial respiration and ROS. *Biochim. Biophys. Acta Bioenergetics* **1837**, 287–295.

Csaszma, I., Andrasi, E., Lasztity, A., Bertalan, E., and Gawlik, D. (2003). Determination of Mo and Mn in human brain samples by different techniques. *J. Analyt. Atomic Spectrom.* **18**, 1082–1087.

Cui, X., and Okayasu, R. (2008). Arsenic accumulation, elimination, and interaction with copper, zinc and manganese in liver and kidney of rats. *Food Chem. Toxicol.* **46**, 3646–3650.

Dikalov, S. I., and Harrison, D. G. (2014). Methods for detection of mitochondrial and cellular reactive oxygen species. *Antioxid. Redox Signal.* **20**, 372–382.

Dimovasili, C., Aschner, M., Plaitakis, A., and Zaganas, I. (2015). Differential interaction of hGDH1 and hGDH2 with manganese: Implications for metabolism and toxicity. *Neurochem. Int.* **88**, 60–65.

Erikson, K. M., Dorman, D. C., Lash, L. H., and Aschner, M. (2007). Manganese inhalation by rhesus monkeys is associated with brain regional changes in biomarkers of neurotoxicity. *Toxicol. Sci.* **97**, 459–466.

Fazakerley, G. V., and Reid, D. G. (1979). Determination of the interaction of ADP and dADP with copper(II), manganese(II) and lanthanide(III) ions by nuclear-magnetic-resonance spectroscopy. *Eur. J. Biochem.* **93**, 535–543.

Food and Nutrition Board. (2001). Dietary Reference Intakes for Vitamin A, Vitamin K, Arsenic, Boron, Chromium, Copper, Iodine, Iron, Manganese, Molybdenum, Nickel, Silicon, Vanadium, and Zinc. Washington D.C: National Academy of Sciences.

Galvani, P., Fumagalli, P., and Santagostino, A. (1995). Vulnerability of mitochondrial complex I in PC12 cells exposed to manganese. *Eur. J. Pharmacol.* **293**, 377–383.

Gao, Z., Huang, K., and Xu, H. (2001). Protective effects of flavonoids in the roots of *Scutellaria baicalensis* Georgi against hydrogen peroxide-induced oxidative stress in HS-SY5Y cells. *Pharmacol. Res.* **43**, 173–178.

Gavin, C. E., Gunter, K. K., and Gunter, T. E. (1999). Manganese and calcium transport in mitochondria: Implications for manganese toxicity. *Neurotoxicology* **20**, 445–453.

Gavin, C. E., Gunter, K. K., and Gunter, T. E. (1992). Mn^{2+} sequestration by mitochondria and inhibition of oxidative phosphorylation. *Toxicol. Appl. Pharmacol.* **115**, 1–5.

Gitler, A. D., Chesi, A., Geddie, M. L., Strathearn, K. E., Hamamichi, S., Hill, K. J., Caldwell, K. A., Caldwell, G. A., Cooper, A. A., Rochet, J. C., *et al.* (2009). Alpha-synuclein is part of a diverse and highly conserved interaction network that includes PARK9 and manganese toxicity. *Nat. Genet.* **41**, 308–315.

Go, Y. M., Craige, S. E., Orr, M., Gernert, K. M., and Jones, D. P. (2009). Gene and protein responses of human monocytes to extracellular cysteine redox potential. *Toxicol. Sci.* **112**, 354–362.

Go, Y. M., Park, H., Koval, M., Orr, M., Reed, M., Liang, Y., Smith, D., Pohl, J., and Jones, D. P. (2010). A key role for mitochondria in endothelial signaling by plasma cysteine/cystine redox potential. *Free Radic. Biol. Med.* **48**, 275–283.

Golub, M. S., Hogrefe, C. E., Germann, S. L., Tran, T. T., Beard, J. L., Crinella, F. M., and Lonnerdal, B. (2005). Neurobehavioral evaluation of rhesus monkey infants fed cow's milk formula, soy formula, or soy formula with added manganese. *Neurotoxicol. Teratol.* **27**, 615–627.

Gordon, J., Amini, S., and White, M. K. (2013). General overview of neuronal cell culture. *Methods Mol. Biol.* **1078**, 1–8.

Gruden, N., and Munic, S. (1987). Effect of iron upon cadmium-manganese and cadmium-iron interaction. *Bull. Environ. Contam. Toxicol.* **38**, 969–974.

Hunt, J. B., and Ginsburg, A. (1981). Manganese ion interaction with glutamine synthetase from *Escherichia coli*: Kinetic and equilibrium studies with xylenol orange and pyridine-2,6-dicarboxylic acid. *Biochemistry* **20**, 2226–2233.

Jones, D. P. (2008). Radical-free biology of oxidative stress, *Am. J. Physiol.* **295**, C849–868.

Jones, D. P. (2002). Redox potential of GSH/GSSG couple: Assay and biological significance. *Methods Enzymol.* **348**, 93–112.

Jones, D. P., Carlson, J. L., Samiec, P. S., Sternberg, P., Jr., Mody, V. C., Jr., Reed, R. L., and Brown, L. A. (1998). Glutathione

measurement in human plasma. Evaluation of sample collection, storage and derivatization conditions for analysis of dansyl derivatives by HPLC. *Clin. Chim. Acta* **275**, 175–184.

Kaludercic, N., FabioDiLisa, S., and Di Lisa, F. (2014). Reactive oxygen species and redox compartmentalization. *Front. Physiol.* **5**, 285.

Karlsson, M., Kurz, T., Brunk, U. T., Nilsson, S. E., and Frennesson, C. I. (2010). What does the commonly used DCF test for oxidative stress really show? *Biochem. J.* **428**, 183–190.

Kitazawa, M., Wagner, J. R., Kirby, M. L., Anantharam, V., and Kanthasamy, A. G. (2002). Oxidative stress and mitochondrial-mediated apoptosis in dopaminergic cells exposed to methylcyclopentadienyl manganese tricarbonyl. *J. Pharmacol. Exp. Ther.* **302**, 26–35.

Kovalevich, J., and Langford, D. (2013). Considerations for the use of SH-SY5Y neuroblastoma cells in neurobiology. *Methods Mol. Biol.* **1078**, 9–21.

Kowaltowski, A. J., de Souza-Pinto, N. C., Castilho, R. F., and Vercesi, A. E. (2009). Mitochondria and reactive oxygen species. *Free Radic. Biol. Med.* **47**, 333–343.

Kwakye, G. F., Paoliello, M. M., Mukhopadhyay, S., Bowman, A. B., and Aschner, M. (2015). Manganese-induced Parkinsonism and Parkinson's disease: Shared and distinguishable features. *Int. J. Environ. Res. Public Health* **12**, 7519–7540.

Lai, J. C., Minski, M. J., Chan, A. W., Leung, T. K., and Lim, L. (1999). Manganese mineral interactions in brain. *Neurotoxicology* **20**, 433–444.

Liccione, J. J., and Maines, M. D. (1988). Selective vulnerability of glutathione metabolism and cellular defense mechanisms in rat striatum to manganese. *J. Pharmacol. Exp. Ther.* **247**, 156–161.

Lin, M. T., and Beal, M. F. (2006). Mitochondrial dysfunction and oxidative stress in neurodegenerative diseases. *Nature* **443**, 787–795.

Lippert, A. R., Dickinson, B. C., and New, E. J. (2015). Imaging mitochondrial hydrogen peroxide in living cells. *Methods Mol. Biol.* **1264**, 231–243.

Liu, Y., Barber, D. S., Zhang, P., and Liu, B. (2013). Complex II of the mitochondrial respiratory chain is the key mediator of divalent manganese-induced hydrogen peroxide production in microglia. *Toxicol. Sci.* **132**, 298–306.

Loranger, S., Zayed, J., and Forget, E. (1994). Manganese contamination in Montreal in relation with traffic density. *Water Air Soil Pollut.* **74**, 385–396.

Lucchini, R., Selis, L., Folli, D., Apostoli, P., Mutti, A., Vanoni, O., Iregren, A., and Alessio, L. (1995). Neurobehavioral effects of manganese in workers from a ferroalloy plant after temporary cessation of exposure. *Scand. J. Work Environ. Health* **21**, 143–149.

Maddirala, Y., Tobwala, S., and Ercal, N. (2015). N-acetylcysteineamide protects against manganese-induced toxicity in SHSY5Y cell line. *Brain Res.* **1608**, 157–166.

Matthews, B. W. (1974). Determination of molecular weight from protein crystals. *J. Mol. Biol.* **82**, 513–526.

Maynard, L. S., and Cotzias, G. C. (1955). The partition of manganese among organs and intracellular organelles of the rat. *J. Biol. Chem.* **214**, 489–495.

Menezes-Filho, J. A., Novaes Cde, O., Moreira, J. C., Sarcinelli, P. N., and Mergler, D. (2011). Elevated manganese and cognitive performance in school-aged children and their mothers. *Environ. Res.* **111**, 156–163.

Milatovic, D., Zaja-Milatovic, S., Gupta, R. C., Yu, Y., and Aschner, M. (2009). Oxidative damage and neurodegeneration in manganese-induced neurotoxicity. *Toxicol. Appl. Pharmacol.* **240**, 219–225.

Miller, S. T., Cotzias, G. C., and Evert, H. A. (1975). Control of tissue manganese: Initial absence and sudden emergence of excretion in the neonatal mouse. *Am. J. Physiol.* **229**, 1080–1084.

Molina, R. M., Phattanarudee, S., Kim, J., Thompson, K., Wessling-Resnick, M., Maher, T. J., and Brain, J. D. (2011). Ingestion of Mn and Pb by rats during and after pregnancy alters iron metabolism and behavior in offspring. *Neurotoxicology* **32**, 413–422.

Murthy, R. C., Lal, S., Saxena, D. K., Shukla, G. S., Ali, M. M., and Chandra, S. V. (1981). Effect of manganese and copper interaction on behavior and biogenic amines in rats fed a 10% casein diet. *Chem.-Biol. Interact.* **37**, 299–308.

Myers, J. E., Fine, J., Ormond-Brown, D., Fry, J., Thomson, A., and Thompson, M. L. (2009). Estimating the prevalence of clinical manganism using a cascaded screening process in a South African manganese smelter. *Neurotoxicology* **30**, 934–940.

Nemoto, S., Takeda, K., Yu, Z. X., Ferrans, V. J., and Finkel, T. (2000). Role for mitochondrial oxidants as regulators of cellular metabolism. *Mol. Cell. Biol.* **20**, 7311–7318.

O'Neal, S. L., and Zheng, W. (2015). Manganese toxicity upon overexposure: A decade in review. *Curr. Environ. Health Rep.* **2**, 315–328.

Oubrahim, H., Stadtman, E. R., and Chock, P. B. (2001). Mitochondria play no roles in Mn(II)-induced apoptosis in HeLa cells. *Proc. Natl. Acad. Sci. USA.* **98**, 9505–9510.

Padua, M., Cavaco, A. M., Aubert, S., Bligny, R., and Casimiro, A. (2010). Effects of copper on the photosynthesis of intact chloroplasts: interaction with manganese. *Physiol. Plant.* **138**, 301–311.

Roede, J. R., Hansen, J. M., Go, Y. M., and Jones, D. P. (2011). Maneb and paraquat-mediated neurotoxicity: Involvement of peroxiredoxin/thioredoxin system. *Toxicol. Sci.* **121**, 368–375.

Roney, N., and Colman, J. (2004). Interaction profile for lead, manganese, zinc, and copper. *Environ. Toxicol. Pharmacol.* **18,** 231–234.

Sies, H. (2014). Role of metabolic H2O2 generation: Redox signaling and oxidative stress. *J. Biol. Chem.* **289**, 8735–8741.

Standridge, J. S., Bhattacharya, A., Succop, P., Cox, C., and Haynes, E. (2008). Effect of chronic low level manganese exposure on postural balance: A pilot study of residents in southern Ohio. *J. Occup. Environ. Med.* **50**, 1421–1429.

Takeda, A. (2003). Manganese action in brain function. *Brain Res. Brain Res. Rev.* **41**, 79–87.

Van Remmen, H., Salvador, C., Yang, H., Huang, T. T., Epstein, C. J., and Richardson, A. (1999). Characterization of the antioxidant status of the heterozygous manganese superoxide dismutase knockout mouse. *Arch. Biochem. Biophys.* **363**, 91–97.

Wasserman, G. A., Liu, X., Parvez, F., Ahsan, H., Levy, D., Factor-Litvak, P., Kline, J., van Geen, A., Slavkovich, V., LoIacono, N. J., *et al.* (2006). Water manganese exposure and children's intellectual function in Araihazar, Bangladesh. *Environ. Health Perspect.* **114**, 124–129.

Weiner, L. M., Backer, J. M., and Rezvukhin, A. I. (1975). Participation of manganese ions complexed with tRNA in the interaction with amino acids and dipeptides. *Biochim. Biophys. Acta* **383**, 316–324.

Winterbourn, C. C. (2014). The challenges of using fluorescent probes to detect and quantify specific reactive oxygen species in living cells. *Biochim. Biophys. Acta* **1840**, 730–738.

Wu, Z., Zhu, Y., Cao, X., Sun, S., and Zhao, B. (2014). Mitochondrial toxic effects of Abeta through mitofusins in the early pathogenesis of Alzheimer's disease. *Mol. Neurobiol.* **50**, 986–996.

Xie, H. R., Hu, L. S., and Li, G. Y. (2010). SH-SY5Y human neuroblastoma cell line: In vitro cell model of dopaminergic neurons in Parkinson's disease. *Chin. Med. J. (Engl.)* **123**, 1086–1092.

Yang, J., Liu, X., Bhalla, K., Kim, C. N., Ibrado, A. M., Cai, J., Peng, T. I., Jones, D. P., and Wang, X. (1997). Prevention of apoptosis by Bcl-2: Release of cytochrome c from mitochondria blocked. *Science* **275**, 1129–1132.

Yao, L., Chen, Q. Y., Xu, X. L., Li, Z., and Wang, X. M. (2013). Interaction of manganese(II) complex with apotransferrin and the apotransferrin enhanced anticancer activities. *Spectrochim. Acta A Mol. Biomol. Spectrosc.* **105**, 207–212.

Yoon, H., Lee, G. H., Kim, D. S., Kim, K. W., Kim, H. R., and Chae, H. J. (2011). The effects of 3, 4 or 5 amino salicylic acids on manganese-induced neuronal death: ER stress and mitochondrial complexes. *Toxicol. In Vitro* **25**, 1259–1268.

Zhang, S., Fu, J., and Zhou, Z. (2004). In vitro effect of manganese chloride exposure on reactive oxygen species generation and respiratory chain complexes activities of mitochondria isolated from rat brain. *Toxicol. In Vitro* **18**, 71–77.

Zhu, Y., Hoell, P., Ahlemeyer, B., Sure, U., Bertalanffy, H., and Krieglstein, J. (2007). Implication of PTEN in production of reactive oxygen species and neuronal death in in vitro models of stroke and Parkinson's disease. *Neurochem. Int.* **50**, 507–516.